

Hydrothermal synthesis and electrochemical properties of a coordination polymer based on dinuclear (Pyrazinyl tetrazolate) Copper(II) cations and β -Octamolybdate Anions

SHAOBIN LI^{a,b}, LI ZHANG^a, HUIYUAN MA^{a,*} and HAIJUN PANG^{a,*}

^aKey Laboratory of Green Chemical Engineering and Technology, College of Heilongjiang Province, College of Chemical and Environmental Engineering, Harbin, University of Science and Technology, Harbin 150040 China

^bCollege of Materials Science and Engineering, Qiqihar University, Qiqihar 161006, China
e-mail: mahy017@163.com; panghj116@163.com

MS received 29 October 2015; revised 20 January 2016; accepted 14 March 2016

Abstract. A hybrid compound $(\text{H}_2\text{bbi})[\text{Cu}_2(\text{pzta})_2(\text{H}_2\text{O})_2][\beta\text{-Mo}_8\text{O}_{26}]$ (**1**) (pztaH = 5-(2-pyrazinyl) tetrazolate, bbi = 1,1'-(1,4-butanediyl)bis(imidazole)), has been hydrothermally synthesized and characterized by elemental analysis, IR spectroscopy and single-crystal X-ray diffraction. In **1**, the $\beta\text{-Mo}_8$ clusters link dinuclear copper (II) complexes as bidentate connectors to form inorganic-organic chains. These chains and the $[\text{H}_2\text{bbi}]^{2+}$ counter-cations are fused together forming layers *via* hydrogen bonding interactions. The electrochemical properties of **1** were studied. The results indicate that **1** has an electrocatalytic activity towards the reduction of iodate ascribed to the Mo-centers.

Keywords. Polyoxometalates; octamolybdate; dinuclear copper complexes; electrochemical properties.

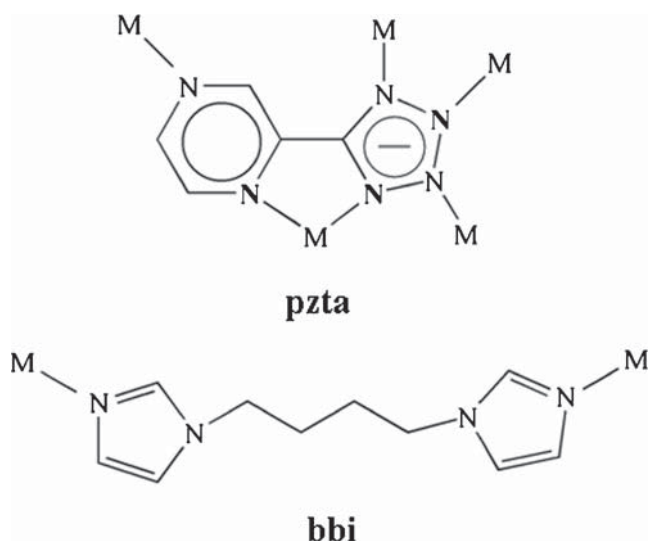
1. Introduction

Polyoxometalates (POMs) are comprised of early-transition metals with d^0 or d^1 electronic configurations (usually Mo^{VI} , W^{VI} , V^{V} , Nb^{V} or Ta^{V}), which have attracted intense attention during the last two decades not only for their remarkable structural and electronic properties, but also for their potential applications in catalysis, electrochemistry and medicine.^{1–6} Coordination polymers are a new generation of solid-state materials that have promising applications in gas storage, catalysis, and porous materials due to their unique structural and functional properties.^{7–9} In virtue of their special properties, it is appealing to construct POM-based coordination polymers, which may combine the advantages of both POMs and coordination polymer, and thus many novel POM-based coordination polymers have been obtained in recent years.^{10–13} Among various POM-based coordination polymers, the coordination polymers based on POMs and dinuclear copper(II) complexes have gained the attention of chemists. Since the first example of coordination polymer based on POMs and dinuclear copper(II) complexes reported by Gutiérrez-Zorrilla and coworkers in 2003,¹⁴ some of this kind of hybrids have been

successfully synthesized.^{15–18} However, to date, such hybrids reported in literature are limited in number. Therefore, the extended studies in this branch are still very significant.

To construct POM-based dinuclear copper(II) compounds, the choice of ligands is vital. The multidentate rigid ligand 5-(2-pyrazinyl) tetrazole (pztaH) possesses flexible coordination modes (scheme 1) due to their six potential nitrogen coordination sites, namely the adjacent four nitrogen atoms of tetrazolyl and the two nitrogen atoms of pyrazinyl, and thus the pzta is readily available to coordinate metal ions for affording polynuclear metal clusters. In our previous work, four POM-based dinuclear/tetranuclear copper(II) compounds constructed by the multidentate pztaH ligand have been synthesized.^{19,20} Moreover, the flexible bbi ligand (scheme 1) as a secondary N-donor ligand, with two terminal nitrogen atoms in imidazole rings and good coordination ability to coordinate metal ions, is easily protonated and thus bbi possesses potential sites for hydrogen bonding towards oxygen atoms of POMs and/or water molecules forming $\text{N-H}\cdots\text{O}$ interactions. Such interactions together with coordination ability of the terminal nitrogen atoms in imidazole rings can effectively extend the structures. Meanwhile, the two imidazole rings can twist freely around the $-\text{CH}_2-$ group

*For correspondence



Scheme 1. View of the potential coordination sites of pzta and bbi ligands.

to meet the requirements of the coordination geometries in the assembly process.

As an extension of our previous work, among the various types of POMs, the octamolybdates (Mo_8) have attracted much attention because of their high reactivities and diverse isomers. In this context, we chose the combination of the multidentate ligand pztaH and the flexible bbi ligand to construct POM-based coordination polymer. A new compound $(\text{H}_2\text{bbi})[\text{Cu}_2(\text{pzta})_2(\text{H}_2\text{O})_2][\beta\text{-Mo}_8\text{O}_{26}]$ (**1**) has been successfully synthesized under hydrothermal conditions. In addition, the electrocatalytic properties of **1** were investigated.

2. Experimental

2.1 Materials and methods

All the chemicals were of reagent grade and used without further purification. Elemental analyses (C, H and N) were performed on a Perkin-Elmer 2400 CHN Elemental Analyzer. The FT-IR spectra were recorded from KBr pellets in the range $4000\text{--}400\text{ cm}^{-1}$ with a Nicolet AVATAR FT-IR360 spectrometer. A CHI660 electrochemical workstation was used for control of the electrochemical measurements and data collection. A conventional three-electrode system was used, with a carbon paste electrode (CPE) as a working electrode, commercial Ag/AgCl as reference electrode and a twisted platinum wire as counter electrode.

2.2 Synthesis of compound **1**

A mixture of $(\text{NH}_4)_6\text{Mo}_7\text{O}_{24}\cdot 4\text{H}_2\text{O}$ (0.37 g, 0.3 mmol), $\text{CuCl}_2\cdot 2\text{H}_2\text{O}$ (0.16 g, 0.9 mmol), pzta (0.059 g, 0.4

mmol), bbi (0.076 g, 0.4 mmol), and H_2O (15 mL) were stirred for 1 h. Then the solution was sealed in a 23 mL Teflon-lined autoclave and heated at 170°C for 3 days with a starting pH = 3.5 adjusted by 1 M HCl. After slow cooling to room temperature, blue block-shaped crystals of **1** were filtered, washed with distilled water and dried at room temperature (46% yield based on Mo). The final pH value of the solution after the reaction was approximated to 3.2. Elemental analysis for $\text{C}_{20}\text{H}_{26}\text{Cu}_2\text{Mo}_8\text{N}_{16}\text{O}_{28}$ (**1**) (1833.14): H, 1.43; C, 13.10; N, 12.23; Cu, 6.93; Mo, 41.87%. Found: H, 1.35; C, 13.19; N, 12.31; Cu, 6.84; Mo, 41.79%.

2.3 X-Ray Crystallographic Study

A single crystal of **1** was carefully selected for X-ray diffraction analysis. Data collection were performed on a Rigaku RAXIS-RAPID instrument equipped with a narrow-focus, 5.4 kW sealed tube X-ray source (graphite e-monochromated $\text{MoK}\alpha$ radiation $\lambda = 0.71073\text{ \AA}$). The data were collected at a temperature of 293 K. The data were processed with the PROCESS-AUTO program. The structure of **1** was solved by Direct Methods

Table 1. Crystal data and structure refinement data for **1**.

Empirical formula	$\text{C}_{20}\text{H}_{26}\text{Cu}_2\text{Mo}_8\text{N}_{16}\text{O}_{28}$
<i>Mr</i>	1833.14
Color, habit	blue, block
Crystal size, mm^3	$0.36 \times 0.32 \times 0.28$
Crystal system; space group	triclinic; $P\bar{1}$
<i>a</i> \AA	9.7012(7)
<i>b</i> \AA	11.1792(8)
<i>c</i> \AA	11.2056(8)
α , deg	118.447(1)
β , deg	95.778(1)
γ , deg	93.443(1)
<i>V</i> , \AA^3	1054.97(13)
<i>Z</i>	1
<i>D</i> _{calcd.} g cm^{-3}	2.88
$\mu(\text{MoK}\alpha)$, mm^{-1}	33.9
<i>F</i> (000), e	870.0
<i>hkl</i> range	$-12 \leq h \leq 12$, $-14 \leq k \leq 13$, $-10 \leq l \leq 14$
Absorption correction	multi-scan
Refl. measured/unique	6576 / 5211
<i>R</i> _{int}	0.0125
Data/parameters	4816 / 334
GoF (<i>F</i> ²)	1.078
<i>R</i> ₁ / <i>wR</i> ₂ [<i>I</i> > 2 σ (<i>I</i>)] ^{a, b}	0.0269 / 0.0725
<i>R</i> ₁ / <i>wR</i> ₂ (all data)	0.0293 / 0.0738
$\Delta\rho_{\text{fin}}$ (max / min), e \AA^{-3}	0.78 / -0.16

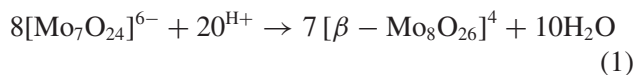
^a $R_1 = \frac{\sum \|F_o\| - |F_c|}{\sum F_o}$;

^b $wR_2 = [\frac{\sum w(F_o^2 - F_c^2)^2}{\sum w(F_o^2)^2}]^{1/2}$

and refined by full-matrix least-squares on F^2 using the SHELXTL-97 crystallographic software package.²¹ Anisotropic displacement parameters were used to refine all non-hydrogen atoms. The organic hydrogen atoms were generated geometrically. The hydrogen atoms of the water molecule in **1** could not be introduced in the refinement but were included in the structure factor calculation. Further details of the X-ray structure analysis are given in table 1. Selected bond lengths and angles are listed in table S1 (in Supplementary Information). Crystal data and structure refinement, bond lengths and angles, and anisotropic displacement parameters have been deposited.

3. Results and Discussion

It is worth noting that Mo_8 could be easily formed *in situ* by using $(\text{NH}_4)_6\text{Mo}_7\text{O}_{24}\cdot 4\text{H}_2\text{O}$ precursor under acid medium.^{22–25} We deduce the conversion pathways of the $[\text{Mo}_7\text{O}_{24}]^{6-}$ anion into the $[\beta\text{-Mo}_8\text{O}_{26}]^{4-}$ anion according to the following acid-base equilibrium (eq. 1):



3.1 Description of the Crystal Structure

The single-crystal X-ray diffraction analysis has shown that **1** consists of one $\beta\text{-}[\text{Mo}_8\text{O}_{26}]^{4-}$ anion (abbreviated as $\beta\text{-Mo}_8$), two Cu cations, two pzta ligands, one

biprotonated bbi ligand and two water molecules (figure 1). The Mo atoms are in +6 oxidation state and the Cu atoms in +2 oxidation state, confirmed by their BVS calculations,²⁶ the coordination environments and green crystal color.

There are three basic subunits in **1**: a dinuclear copper cation $[\text{Cu}_2(\text{pzta})_2(\text{H}_2\text{O})_2]^{2+}$ (**I**), a $\beta\text{-Mo}_8$ anion (**II**) and a biprotonated GTG conformation $[\text{H}_2\text{bbi}]^{2+}$ cation (**III**) (G = gauche, T = trans) (figure 2). In subunit **I**, there is one crystallographically unique Cu cation, and showing a five-coordination in a rectangular pyramidal geometry achieved by three N atoms from two pzta ligands, as well as two O atoms from a $\beta\text{-Mo}_8$ cluster and one coordinated water molecule. The bond lengths and angles around the Cu ions are in the ranges of 1.965(3)–2.038(3) Å (Cu–N), 1.958(3)–2.315(2) Å (Cu–O), 94.27(11)–172.00(11)° (N–Cu–N), and 89.37(10)–171.96(12)° (N–Cu–O). All of these bond lengths and bond angles are within the normal ranges observed in other Cu(II)-containing complexes.²⁷ By these coordination modes, a dinuclear copper(II) complex is formed (figure 2a), in which the distance of two copper atoms ($\text{Cu1} \cdots \text{Cu1}^{\#}$) is 4.009 Å.

The dinuclear copper(II) complex shares its connecting nodes with neighboring $\beta\text{-Mo}_8$ clusters giving rise to an inorganic-organic chain. The inorganic-organic chains and the $[\text{H}_2\text{bbi}]^{2+}$ counter-cations are fused together to form layers with windows *ca.* 11.179×16.131 Å *via* hydrogen bonding interactions ($\text{C10-H10} \cdots \text{O4} = 3.28$ Å, $\text{C9-H9} \cdots \text{O8} = 3.36$ Å) (figures 2c and 2d). From a topological view, if each

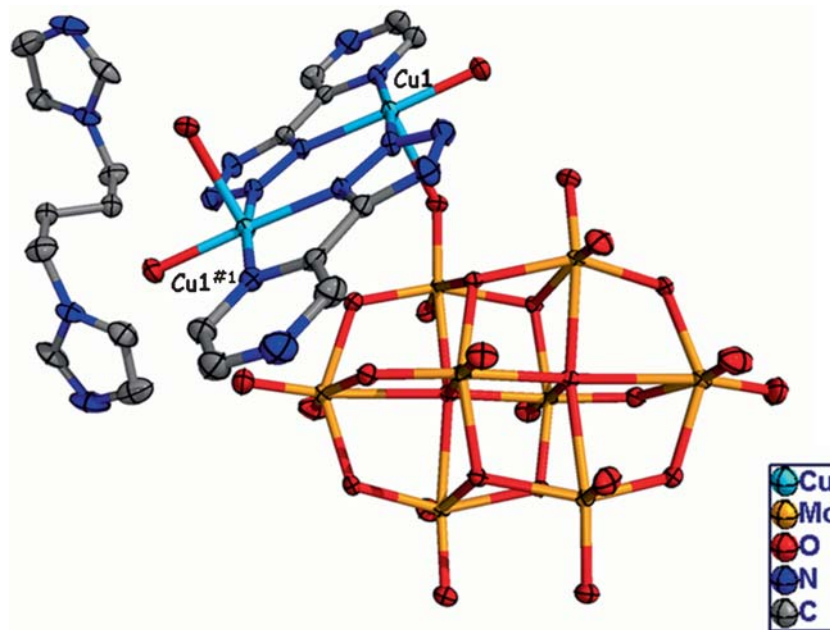


Figure 1. ORTEP drawing of **1** with displacement ellipsoids set at 50% probability. Hydrogen atoms are omitted for clarity. (Symmetry code: #1, $-x, -y, -z$).

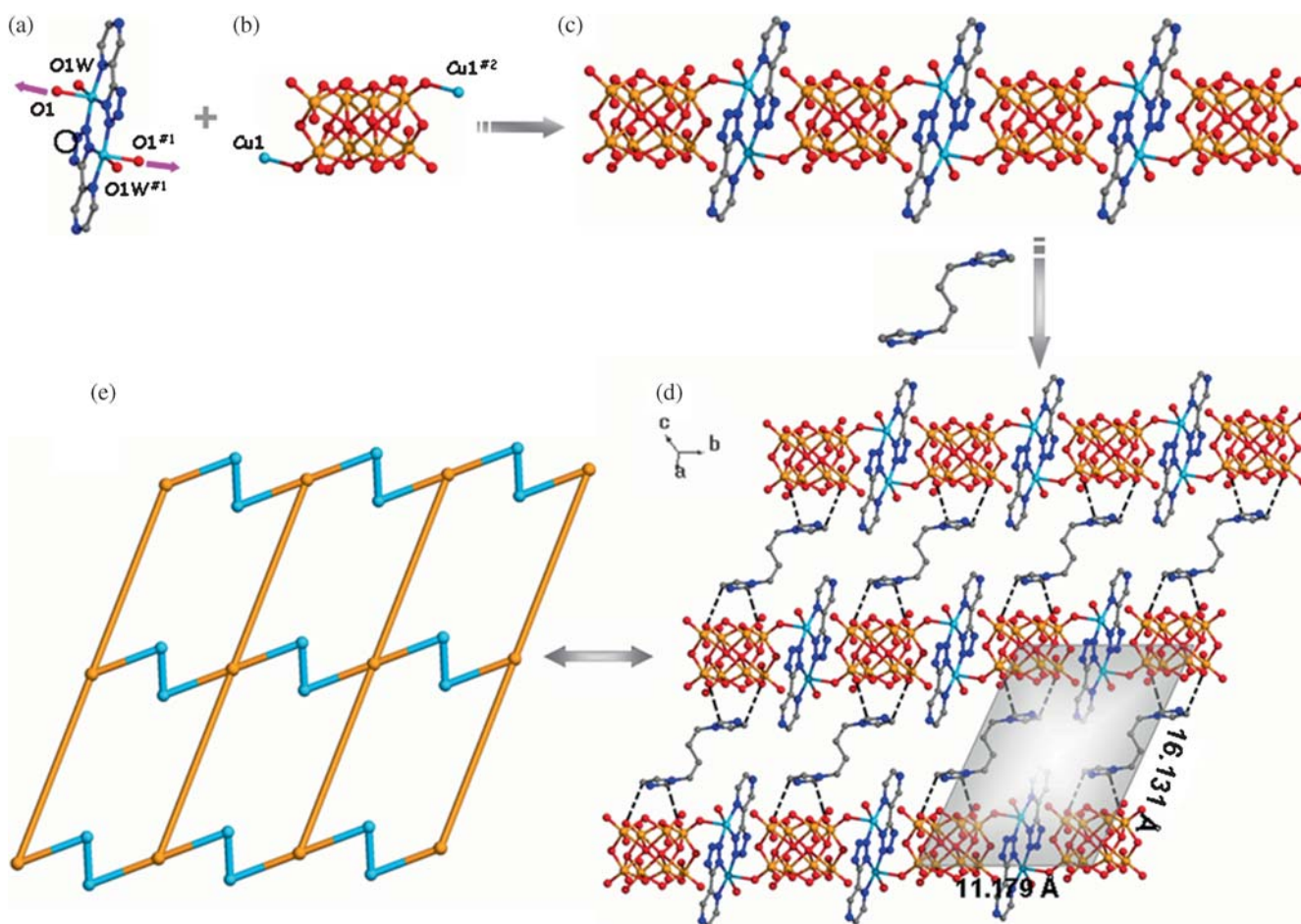


Figure 2. (a) A dinuclear $[\text{Cu}_2(\text{pzta})_2(\text{H}_2\text{O})_2]^{2+}$ cation; (b) a connected $\beta\text{-Mo}_8$ cluster; (c) an inorganic-organic chain and free bbi ligands; (d) a layer formed with the cations; (e) the topology of the layer. (symmetry code: #1, $-x, -y, -z$; #2, $-x, 1-x, -z$).

$\beta\text{-Mo}_8$ anion is considered as a 4-connected node and each Cu cation as a 2-connected node, the structure of **1** is a novel (4, 2)-connected framework with $(4^4 \cdot 12^2)$ topology (figure 2e).

3.2 IR spectrum

The IR spectrum of compound **1** (figure S1 in Supplementary Information) exhibits characteristic peaks at 953, 881, 829 and 660 cm^{-1} , which are attributed to $\nu(\text{Mo}=\text{O}_t)$, $\nu(\text{Mo}-\text{O}_b-\text{Mo})$ and $\nu(\text{Mo}-\text{O}_c-\text{Mo})$, respectively.²⁸ The bands in the region of 1596 to 1101 cm^{-1} are ascribed to vibrations of the pzta and bbi components. The broad band at 3235 cm^{-1} is associated with the water molecules.

3.3 Electrochemical properties

POMs possess the ability of undergoing reversible multi-electron redox processes,²⁹ which make them very attractive for chemically modified electrodes to be used in electrocatalytic studies. Since the title compound is

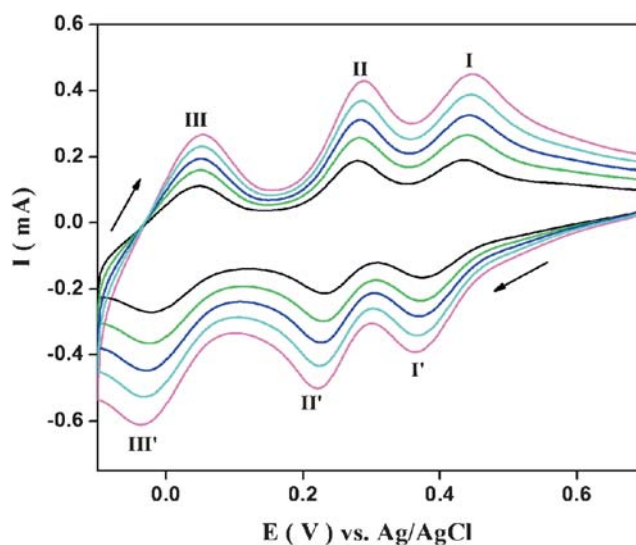


Figure 3. Cyclic voltammograms for **1**-CPE in 1 M H_2SO_4 solution at different scan rates (from inner to outer): 50, 100, 150, 200, 250 $\text{mV} \cdot \text{s}^{-1}$.

insoluble in water and common organic solvents, a bulk-modified carbon paste electrode (CPE) is the optimal choice to study its electrochemical properties.³⁰

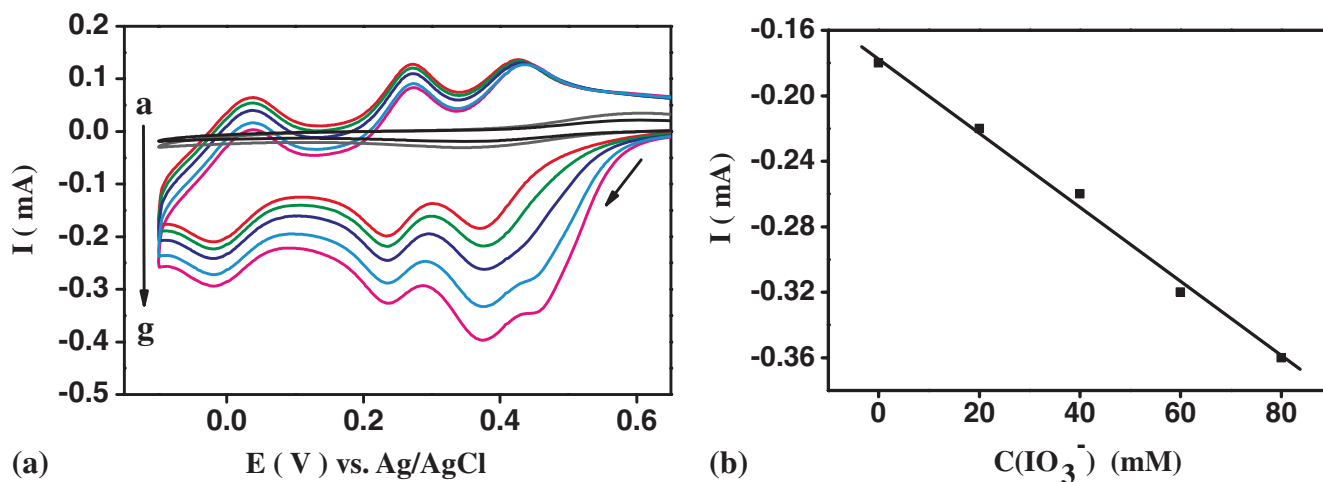


Figure 4. (A) Cyclic voltammograms: (a) bare CPE in 1 M H₂SO₄ solution, (b) bare CPE in 1 M H₂SO₄ and IO₃⁻ (80 mM), (c-g) **1**-CPE in 1 M H₂SO₄ solution containing IO₃⁻ (c) 0, (d) 20, (e) 40, (f) 60 and (g) 80 mM. Scan rate: 50 mV s⁻¹. (B) Linear dependence of the cathodic catalytic current of wave I-I' on the IO₃⁻ concentration.

The cyclic voltammograms (CV) for **1**-CPE in 1 M H₂SO₄ aqueous solution at different scan rates are presented in figure 3. It can be seen clearly that three reversible redox peaks (I-I', II-II' and III-III') appear in the potential range from +0.7 to -0.1 V vs. Ag/AgCl. The mean peak potentials $E_{1/2} = (E_{pa} + E_{pc})/2$ are 0.02 V (I), 0.25 V (II) and 0.42 V (III) (scan rate: 50 mV·s⁻¹), which are all ascribed to three consecutive two-electron redox processes of Mo.³¹⁻³³

POMs have been exploited extensively in electrocatalytic reactions and further with possible applications as biosensors or in fuel cells.³⁴ Here, the reduction of iodate (IO₃⁻) was chosen as a test reaction to study the electrocatalytic activity of **1**. As shown in figure 4A, it displays good electrocatalytic activity toward the reduction of IO₃⁻ in 1 M H₂SO₄ solution. With the addition of IO₃⁻, the cathodic peak I' substantially increased, while the corresponding anodic peak currents decreased. Meanwhile, an extra CV peak (at ~ 0.45 V) in the CV of **1**-CPE in the presence of iodate (60 mM) has emerged. The reason for this appearance may be that the reduction peak I' is split. This phenomenon could be observed in the previous work.^{19,35} In our work, this extra peak should be identified as I''. The peak potentials $E_{1/2}$ are 0.029 V (I), 0.27 V (II) and 0.44 V (III) (IO₃⁻: 80 mM), which are almost corresponding with peak potentials $E_{1/2}$ (without IO₃⁻). Thus, the peak potentials indicate stability in the catalytic process.³⁶ Figure 4B shows the relationship between the first cathodic current and the concentration of IO₃⁻. The electrocatalytic efficiency of **1**-CPE (based on a rough calculation using catalytic efficiency (CAT) formula)³⁷ towards the reduction of IO₃⁻ was ca. 110% at 1 M H₂SO₄ containing 80 mM IO₃⁻, which suggests that

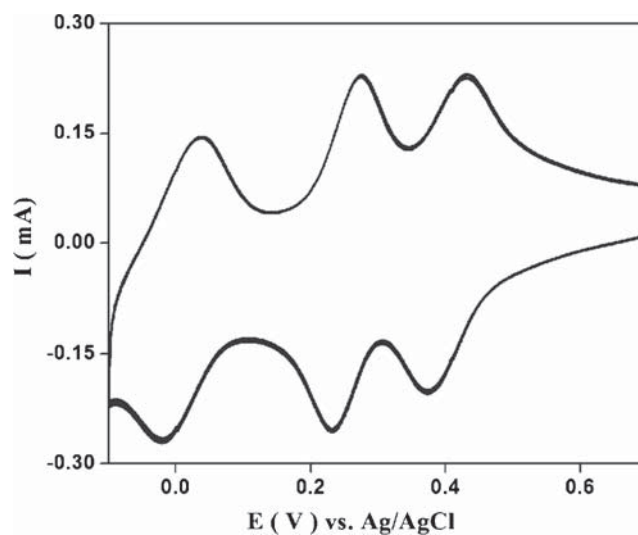


Figure 5. 40 consecutive CV cycles of the **1**-CPE at the scan rate of 50 mV·s⁻¹.

1 has potential usefulness for the detection of IO₃⁻. Furthermore, the stability experiment for **1**-CPE has been investigated by cyclic voltammetry scanning for 40 cycles in 1 M H₂SO₄ solution, respectively. As shown in figure 5, it can be seen that the electrode exhibits almost no loss in the current signal after 40 cycles, which suggests that the catalyst of **1**-CPE has high stability.

4. Conclusion

To sum up, a new POM-based dinuclear copper (II) coordination polymer (H₂bbi)[Cu₂(pzta)₂(H₂O)₂][β-Mo₈O₂₆] (**1**) has been synthesized by the hydrothermal reaction. In the structure of **1**, the biprotonated bbi

ligands, acting as counter-cations, extend the structure by hydrogen bonding interactions. Furthermore, the electrochemical properties of **1** were studied, which indicate that **1** has good electrocatalytic activity towards reduction of iodate. Synthesis and property investigation on other POM-based coordination polymers constructed by dinuclear copper (II) complex are continuing in our group.

Supplementary Information (SI)

CIF file containing complete information on the structure was deposited with CCDC deposition number 992478, which is available free upon request from The Cambridge Crystallographic Data Centre via www.ccdc.cam.ac.uk/data_request/cif. The table of selected bond lengths and angles and the IR spectrum of compound **1** are given in supplementary information available at www.ias.ac.in/chemsci.

Acknowledgements

This work was financially supported by the NSF of China (21371041, 51572063), innovative research team of green chemical technology in university of Heilongjiang Province, China (2014TD007), and the science and technology innovation foundation of Harbin (2014RFXXJ076).

References

- Coronado E and Gómez-García C J 1998 *Chem. Rev.* **98** 273
- Müller A and Kögerler P 2000 *Coord. Chem. Rev.* **199** 335
- Han Q X, He C, Zhao M, Qi B, Niu J Y and Duan C Y 2013 *J. Am. Chem. Soc.* **135** 10186
- Yin Q S, Tan J M, Besson C, Geletii Y V, Musaev D G, Kuznetsov A E, Luo Z, Hardcastle K I and Hill C L 2010 *Science* **328** 342
- Hill C L 1998 *Chem. Rev.* **98** 1
- Han X B, Li Y G, Zhang Z M, Tan H Q, Lu Y and Wang E B 2015 *J. Am. Chem. Soc.* **137** 5486
- Yaghi O M, Keeffe M O, Ockwig N W, Chae H K, Eddaoudi M and Kim J 2003 *Nature* **423** 705
- Rowsell J L, Spencer E C, Eckert J, Howard J A and Yaghi O M 2005 *Science* **309** 1350
- Custelcean R 2014 *Chem. Soc. Rev.* **43** 1813
- Wang S S and Yang G Y 2015 *Chem. Rev.* **115** 4892
- Vaddypally S and Samar K D 2005 *Inorg. Chem.* **44** 8846
- Monima S, Tanmay C and Samar K D 2011 *Dalton Trans.* **40** 2954
- Du D Y, Yan L K, Su Z M, Li S L, Lan Y Q and Wang E B 2013 *Coord. Chem. Rev.* **257** 702
- Reinoso S, Vitoria P, Lezama L, Luque A and Gutiérrez-Zorrilla J M 2003 *Inorg. Chem.* **42** 3709
- Reinoso S, Vitoria P, Gutiérrez-Zorrilla J M, Lezama L S, Felices L and Beitia J I 2005 *Inorg. Chem.* **44** 9731
- Cao R G, Liu S X, Xie L H, Pan Y B, Cao J F, Ren Y H and Xu L 2007 *Inorg. Chem.* **46** 3541
- Yu F, Kong X J, Zheng Y Y, Ren Y P, Long L S, Huang R B and Zheng L S 2009 *Dalton Trans.* 9503
- Han Q X, Ma P T, Zhao J W, Wang J P and Niu J Y 2011 *Inorg. Chem. Commun.* **14** 767
- Li S B, Ma H Y, Pang H J, Zhang Z F, Yu Y, Liu H and Yu T T 2014 *Cryst. Eng. Comm.* **16** 2045
- Li S B, Ma H Y, Pang H J, Li Z and Zhang Z F 2014 *Inorg. Chem. Commun.* **44** 15
- Sheldrick GM (2000) shelxtl (version 6.1) (Bruker Analytical, X-ray Instruments Inc. : Madison, Wisconsin)
- Li S L, Lan Y Q, Ma J F, Yang J, Wang X H and Su Z M 2007 *Inorg. Chem.* **46** 8283
- Allis D G, Burkholder E and Zubieta J 2004 *Polyhedron* **23** 1145
- Wu H, Yang J, Liu Y Y and Ma J F 2012 *Cryst. Growth Des.* **12** 2272
- Lan Y Q, Li S L, Wang X L, Shao K Z, Su Z M and Wang E B 2008 *Inorg. Chem.* **47** 529
- Brown I D and Altermatt D 1985 *Acta Crystallogr. B* **41** 244
- Sha J Q, Peng J, Zhang Y, Pang H J, Tian A X, Zhang P P and Liu H 2009 *Cryst. Growth Des.* **9** 1708
- Klemperer W G and Shum W 1976 *J. Am. Chem. Soc.* **98** 8291
- Xi X D, Wang G, Liu B F and Dong S J 1995 *Electrochim. Acta* **40** 1025
- Han Z G, Zhao Y L, Peng J, Feng Y H, Yin J N and Liu Q 2005 *Electroanalysis* **17** 1097
- Dong S J and Wang B X 1992 *Electrochim. Acta* **37** 11
- Dai L M, You W S, Wang E B, Wu S X, Su Z M, Du Q H, Zhao Y and Fang Y 2009 *Cryst. Growth Des.* **9** 110
- Sha J Q, Liang L Y, Sun J W, Tian A X, Yan P F, Li G M and Wang C 2012 *Cryst. Growth Des.* **12** 894
- Keita B, Oliveira P D, Nadjo L and Kortz U 2007 *Chem. Eur. J.* **13** 5480
- Qu Z K, Yu K, Zhao Z F, Su Z H, Sha J Q, Wang C M and Zhou B B 2014 *Dalton Trans.* **43** 6744
- Qin Q S, Du D Y, Guan W, Bo X J, Li Y F, Guo L P, Su Z M, Wang Y Y, Lan Y Q and Zhou H C 2015 *J. Am. Chem. Soc.* **137** 7169
- Keita B, Belhouari A, Nadjo L and Contant R 1995 *J. Electroanal. Chem.* **381** 243